

MASSACHUSETTS INSTITUTE OF TECHNOLOGY  
ARTIFICIAL INTELLIGENCE LABORATORY

A.I. Memo 498

October, 1978

**CALCULATING THE REFLECTANCE MAP**

Berthold K. P. Horn  
Robert W. Sjoberg

Abstract

It appears that the development of machine vision may benefit from a detailed understanding of the imaging process. The reflectance map, showing scene radiance as a function of surface gradient, has proved to be helpful in this endeavor. The reflectance map depends both on the nature of the surface layers of the objects being imaged and the distribution of light sources. Recently, a unified approach to the specification of surface reflectance in terms of both incident and reflected beam geometry has been proposed. The reflecting properties of a surface are specified in terms of the bidirectional reflectance-distribution function (BRDF).

Here we derive the reflectance map in terms of the BRDF and the distribution of source radiance. A number of special cases of practical importance are developed in detail. The significance of this approach to the understanding of image formation is briefly indicated.

This report describes research done at the Artificial Intelligence Laboratory of the Massachusetts Institute of Technology. Support for the Laboratory's artificial intelligence research is provided in part by the Advanced Research Projects Agency of the Department of Defense under Office of Naval Research contract N00014-75-C-0643.

## TABLE OF CONTENTS

|   |    |
|---|----|
| 1. The Reflectance Map . . . . .  | 3  |
| 2. Microstructure of Surfaces . . . . .                                       | 3  |
| 3. Radiometry . . . . .   | 7  |
| 4. The Bidirectional Reflectance-Distribution Function . . . . .              | 9  |
| 5. Integrals Over Solid Angles and Projected Solid Angles . . . . .           | 10 |
| 6. Perfectly Diffuse Reflectance . . . . .                                    | 12 |
| 7. Collimated Sources and the Dirac Delta-Function . . . . .                  | 12 |
| 8. Perfectly Specular Reflectance . . . . .                                   | 13 |
| 9. Analysis of Image-Forming System . . . . .                                 | 14 |
| 10. Viewer-Oriented Coordinate System . . . . .                               | 16 |
| 11. The Surface Normal . . . . .  | 17 |
| 12. Relationship Between Local and View-Oriented Coordinate Systems . . . . . | 18 |
| 13. Scene Radiance . . . . .  | 20 |
| 14a. Collimated Source, Lambertian Reflectance . . . . .                      | 21 |
| 14b. Uniform Source, Lambertian Reflectance . . . . .                         | 22 |
| 14c. Hemispherical Uniform Source, Lambertian Reflectance . . . . .           | 22 |
| 15a. Collimated Source, Specular Reflectance . . . . .                        | 24 |
| 15b. Uniform Source, Specular Reflectance . . . . .                           | 26 |
| 15c. Hemispherical Uniform Source, Specular Reflectance . . . . .             | 26 |
| Summary and Conclusions . . . . .   | 26 |
| Acknowledgements . . . . .  | 27 |
| References . . . . .  | 27 |

## §1. THE REFLECTANCE MAP

The apparent "brightness" of a surface patch depends on the orientation of the patch relative to the viewer and the light sources. Different surface elements of a non-planar object will reflect different amounts of light towards an observer as a consequence of their differing attitude in space. A smooth opaque object will thus give rise to a shaded image, one in which brightness varies spatially, even though the object may be illuminated evenly and covered by a uniform surface layer. This shading provides important information about the object's shape and has been exploited in machine vision [1-8].

A convenient representation for the relevant information is the "reflectance map" [4, 6]. The reflectance map,  $R(p, q)$ , gives scene radiance as a function of surface gradient  $(p, q)$  in a viewer-centered coordinate system. If  $z$  is the elevation of the surface above a reference plane lying perpendicular to the optical axis of the imaging system, and if  $x$  and  $y$  are distances in this plane measured parallel to orthogonal coordinate axes in the image, then  $p$  and  $q$  are the first partial derivatives of  $z$  with respect to  $x$  and  $y$ :

$$p = \partial z / \partial x \quad \text{and} \quad q = \partial z / \partial y$$

The reflectance map is usually depicted as a series of contours of constant scene radiance (Fig. 1). It can be measured directly using a goniometer-mounted sample, or indirectly from the image of an object of known shape. Alternatively, a reflectance map may be calculated if properties of the surface material and the distribution of light sources are given. One purpose of this paper is to provide a systematic approach to this latter endeavor. Another is to derive the relationship between scene radiance and image irradiance in an imaging system. This is relevant to machine vision since gray-levels are quantized measurements of image irradiance.

## §2. MICROSTRUCTURE OF SURFACES

When a ray of light strikes the surface of an object it may be absorbed, transmitted, or reflected. If the surface is flat and the underlying material homogeneous, the reflected ray will lie in the plane formed by the incident ray and the surface normal and will make an angle with the local normal equal to the angle between the incident ray and the local normal. This is referred to as "specular," "metallic," or "dielectric" reflection. Objects with surfaces of this kind form virtual images of surrounding objects.

Many surfaces are not perfectly flat on a microscopic scale and thus scatter parallel incident rays into a variety of directions (Fig. 2a). If deviations of the local surface

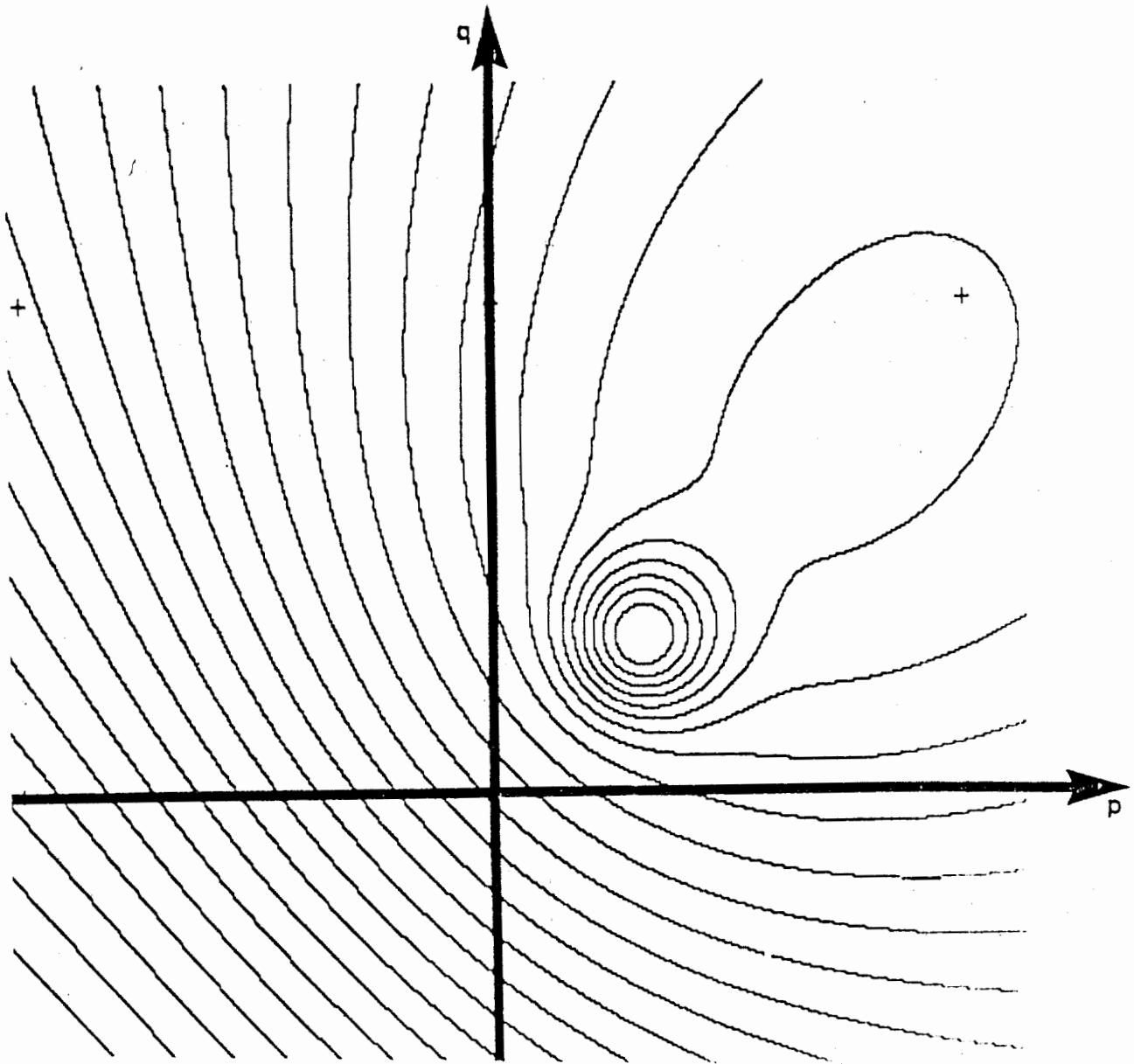


*FIGURE 1:* A typical reflectance map for a surface, with both a glossy and a matte component of reflection, illuminated by a point source. The coordinates are surface slope in the  $x$  and  $y$  directions, and the curves shown are contours of constant scene radiance.

normals from the average are small, most of the rays will lie near the direction for ideal specular reflection and contribute to a surface "shine" or "gloss."

Other surface layers are not homogeneous on a microscopic scale, and thus scatter light rays which penetrate the surface by refraction and reflection at boundaries between regions with differing refractive indices (Fig. 2b). Scattered rays may re-emerge near the point of entry with a variety of directions and so contribute to "diffuse," "flat," or "matte" reflection. Snow and layers of white paint are examples of surfaces with this kind of behavior. Frequently both effects occur in surface layers, with some rays reflected at the nearly flat outer surface of the object, while others penetrate deeper and re-emerge after multiple refractions and reflections in the inhomogeneous interior.

The distribution of reflected light in each case above depends on the direction of incident rays and the details of the microstructure of the surface layer. Naturally, what constitutes microstructure depends on one's point of view. Surface structures not resolved in a particular imaging situation are taken here to be microstructure. When viewing the moon through a telescope, for example, smaller "hillocks" and "craterlets" are part of this microstructure. This consideration leads to more complicated models of interaction of light with surfaces than those discussed so far. It is possible, for instance, to consider an undulating surface covered with a material which in itself already has complicated reflecting behavior (Fig. 2c).

Reflectance is not altered by rotating a surface patch about its normal when there is no asymmetry or preferred direction to either the pattern of surface undulations or the distribution of sub-surface inhomogeneities. Many surface layers behave this way and permit a certain degree of simplification of the analysis. Exceptions are such things as diffraction gratings, iridescent plumage and the mineral called "tiger eye." These all have a distinct directionality in their surface microstructure and will not be considered here any further.

Considerable attention has been paid to the reflective properties of various surface layers. Some researchers have concentrated on the experimental determination of surface reflectance properties [9-21]. At the same time, many models have been developed for surface layers based on some of the considerations presented above [22-35]. Models often are too simple to be realistic, or too complicated to yield solutions in closed form. In the latter case, Monte-Carlo methods can be helpful, although they lead only to numerical specification of the reflecting behavior. Purely phenomenological models of reflectance have found favor in the computer graphics community [36, 37, 38]. Several books have appeared describing the uses of reflectance measurements in determining basic optical properties of the materials involved [39, 40, 41]. Attention has been paid, too, to the problem of making precise the definitions of reflectance and related concepts [42, 43].

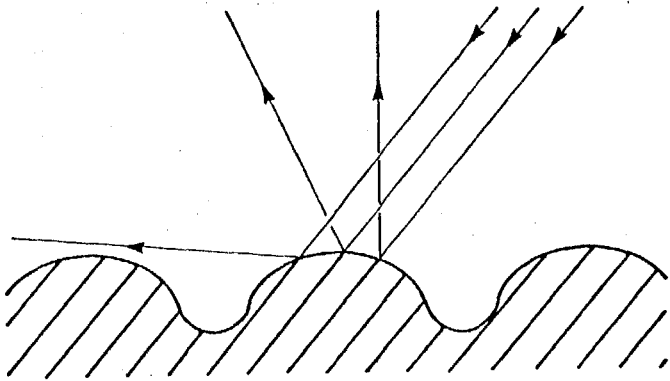


**FIGURE 2a:** Undulations in a specularly reflecting surface causing scattering of incident rays into a variety of directions. The surface will not appear specular if it is imaged on a scale where the surface undulations are not resolved. It may instead have a glossy appearance.

**FIGURE 2b:** Inhomogeneities in refractive index of surface layer components cause incident rays to be scattered into a variety of directions upon reflection. This kind of surface micro-structure gives rise to matte reflection.

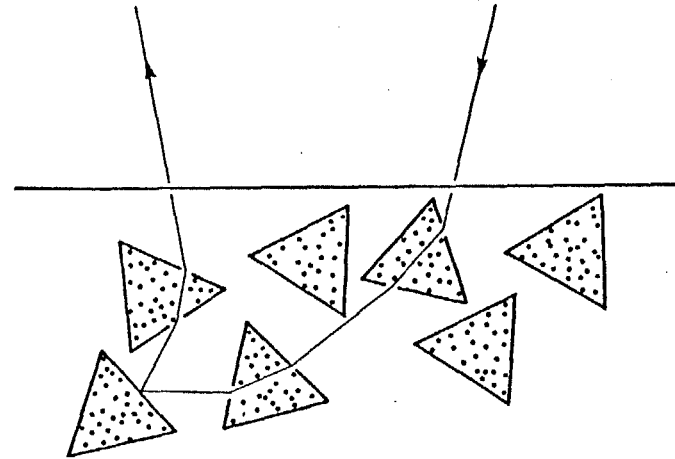
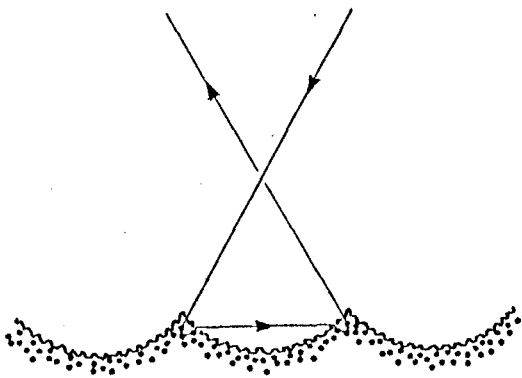


**FIGURE 2c:** Compound surface illustrating more complex model of interaction of light rays with surface microstructure.



### §3. RADIOMETRY

A modern, precise nomenclature for radiometric terms has been promoted by a recent NBS publication [43]. The following short table gives the terms, preferred symbols and unit dimensions of the radiometric concepts we will have occasion to use for the development presented here:

#### RADIOMETRIC CONCEPTS

|                   |  |   |
|-------------------|--|---|
| Radiant flux      | $\Phi$   | [W]                                       |
| Radiant Intensity | $I = d\Phi/d\omega$                                  | [W • sr <sup>-1</sup> ]                   |
| Irradiance        | $E = d\Phi/dA$                                       | [W • m <sup>-2</sup> ]                    |
| Radiant Exitance  | $M = d\Phi/dA$                                       | [W • m <sup>-2</sup> ]                    |
| Radiance          | $L = d^2\Phi / (dA \cdot \cos \theta \cdot d\omega)$ | [W • m <sup>-2</sup> • sr <sup>-1</sup> ] |

Radiant flux,  $\Phi$ , is the power propagated as optical electromagnetic radiation and is measured in watts [W]. The radiant intensity,  $I$ , of a source is the exitant flux per unit solid angle and is measured in watts per steradian [W • sr<sup>-1</sup>]. The total flux emitted by a source is the integral of radiant intensity over the full sphere of possible directions ( $4\pi$  steradians). The irradiance,  $E$ , is the incident flux density, while radiant exitance,  $M$ , is the exitant flux density, both measured in watts per square meter of surface [W • m<sup>-2</sup>]. The total radiant exitance equals the total irradiance if the surface reflects all incident light, absorbing and transmitting none.

The radiance,  $L$ , is the flux emitted per unit *foreshortened* surface area per unit solid angle. Radiance is measured in watts per square meter per steradian [W • m<sup>-2</sup> • sr<sup>-1</sup>]. It can equivalently be defined as the flux emitted per unit surface area per unit *projected* solid angle. Radiance is an important concept since the apparent brightness of a surface patch is related to its radiance. Specifically, image irradiance will be shown to be proportional to scene radiance.

Radiance is a directional quantity. If the angle between the surface normal and the direction of exitant radiation is  $\theta$ , then the term "foreshortened area" stands for the actual surface area times the cosine of this angle  $\theta$ . Similarly the "projected solid angle" stands for the actual solid angle times the cosine of the angle  $\theta$ . Here we will use the symbol  $\omega$  to denote a solid angle, while  $\Omega$  will be used to denote a *projected* solid angle.

If  $d\omega$  and  $d\Omega$  are corresponding infinitesimal solid angles and projected solid angles respectively, then

$$d\Omega = d\omega \cdot \cos \theta$$

The following example (Fig. 3) will illustrate some of these ideas. Consider a source of radiation with intensity  $I$  in the direction of a surface patch of area  $dA$ , oriented with its surface normal making angle  $\theta$  with the line connecting the patch to the source. In fact, as seen from the source, it appears only as large as a patch of area  $dA \cdot \cos \theta$  would when oriented perpendicular to this line. The corresponding solid angle is simply the area of this equivalent patch divided by the square of the distance from the source to the patch. Thus,

$$d\omega = dA \cdot \cos \theta / r^2 \quad [\text{sr}]$$

The flux intercepted then is

$$d\Phi = I \cdot d\omega = I \cdot dA \cdot \cos \theta / r^2 \quad [\text{W}]$$

The irradiance of the surface is just the incident flux divided by the area of the surface patch.

$$E = d\Phi/dA = I \cdot \cos \theta / r^2 \quad [\text{W} \cdot \text{m}^{-2}]$$

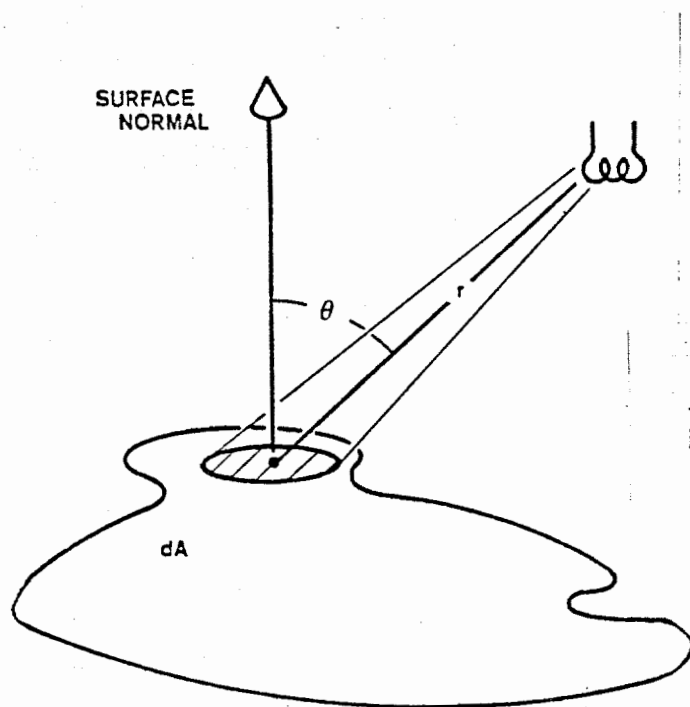


FIGURE 3: Point source illuminating a surface, illustrating basic radiometric concepts.



#### §4. THE BIDIRECTIONAL REFLECTANCE-DISTRIBUTION FUNCTION

The Bidirectional Reflectance-Distribution Function (BRDF) was recently introduced by Nicodemus, Richmond, Hsia, Ginsberg, and Limperis [43] as a unified notation for the specification of reflectance in terms of both incident- and reflected-beam geometry. The BRDF is denoted by the symbol  $f_r$  and captures the information about how "bright" a surface will appear, viewed from a given direction, when it is illuminated from another given direction. To be more precise, it is the ratio of reflected radiance  $dL_r$  in the direction towards the viewer to the irradiance  $dE_i$  in the direction towards a portion of the source. In symbols,

$$f_r(\theta_i, \phi_i; \theta_r, \phi_r) = dL_r(\theta_i, \phi_i; \theta_r, \phi_r; E_i) / dE_i(\theta_i, \phi_i) \quad [\text{sr}^{-1}]$$

Here,  $\theta$  and  $\phi$  together indicate a direction, the subscript  $i$  denoting quantities associated with incident radiant flux, while the subscript  $r$  indicates quantities associated with reflected radiant flux [43].

The geometry is as depicted in the figure (Fig. 4). A surface-specific coordinate system is erected with one axis along the local normal to the surface and another defining an arbitrary reference direction in the local tangent plane. Directions are specified by polar angle  $\theta$  (colatitude) measured from the local normal and azimuth angle  $\phi$  (longitude) measured anti-clockwise from the reference direction in the surface. In general, incident flux may arrive from many portions of extended sources, so incident radiance  $L_i(\theta_i, \phi_i)$  is a function of direction. If we consider the component of flux  $d\Phi_i$  arriving on the surface patch of area  $dA$  from an infinitesimal solid angle  $d\omega_i$  in the direction  $(\theta_i, \phi_i)$  we obtain

$$d\Phi_i = L_i \cdot \cos \theta_i \cdot d\omega_i \cdot dA = L_i \cdot d\Omega_i \cdot dA = dE_i \cdot dA$$

where  $dE_i = L_i \cdot \cos \theta_i \cdot d\omega_i$  is the incident irradiance contributed by the portion of the source found in the solid angle  $d\omega_i$  in the direction  $(\theta_i, \phi_i)$ . Similarly, the radiant flux emitted into an infinitesimal solid angle  $d\omega_r$  in the direction  $(\theta_r, \phi_r)$ :

$$d^2\Phi_r = dL_r \cdot \cos \theta_r \cdot d\omega_r \cdot dA = dL_r \cdot d\Omega_r \cdot dA$$

where  $dL_r(\theta_r, \phi_r)$  is the radiance in the direction  $(\theta_r, \phi_r)$  due to the reflection of the flux incident from direction  $(\theta_i, \phi_i)$ . The notation  $dX$ , where  $X$  is one of the radiometric quantities introduced in §3, will always denote a *directional* quantity, that is, one which depends on either the incident or exitant direction. The notation  $d^2X$  will mean a *bidirectional* quantity, which depends on *both* the incident and exitant directions. Thus, the incident flux  $d\Phi_i$  depends only on the direction of incidence, but the exitant flux  $d^2\Phi_r$  depends on both the direction of emittance and (implicitly) on the direction of incidence.

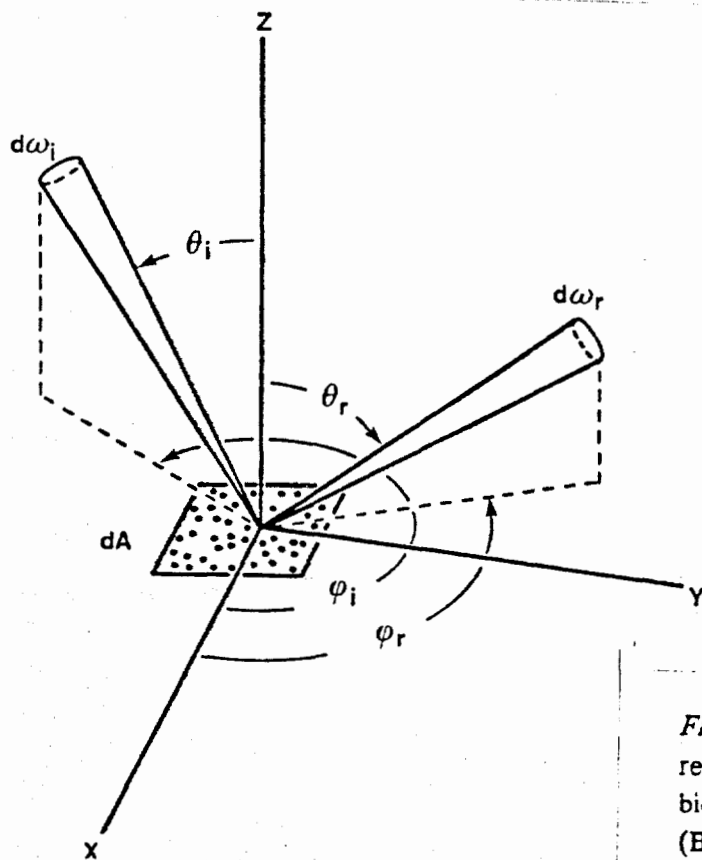


FIGURE 4: Local geometry of incident and reflected rays needed for the definition of the bidirectional reflectance-distribution function (BRDF). Redrawn from [43].

From these values of incident and exitant flux, the BRDF is defined as follows:

$$f_r(\theta_i, \phi_i; \theta_r, \phi_r) = (d^2\Phi_r/d\Omega_r) / d\Phi_i = dL_r/dE_i$$

and thus has dimension inverse steradian [ $\text{sr}^{-1}$ ]. The BRDF allows one to obtain reflectance for any defined incident and reflected ray geometry simply by integrating over the specified solid angles [43].

## §5. INTEGRALS OVER SOLID ANGLES AND PROJECTED SOLID ANGLES

The admitting aperture of an imaging system may occupy a significant solid angle when seen from the point of view of the objects being imaged. We will furthermore have to deal with extended sources. In both cases it is necessary to integrate various quantities over solid angles or projected solid angles. This can be accomplished by

double-integration with respect to the polar and azimuth angles (Fig. 5). If  $X$  is the quantity to be integrated, we have

$$\int_{\omega} X d\omega = \int_{-\pi}^{\pi} \int_0^{\pi/2} X \sin \theta d\theta d\phi$$

and

$$\int_{\Omega} X d\Omega = \int_{-\pi}^{\pi} \int_0^{\pi/2} X \cos \theta \sin \theta d\theta d\phi$$

If for example  $X = 1$  and the region of integration is the hemisphere above the object's surface, then

$$\int_{\omega} X d\omega = \int_{-\pi}^{\pi} \int_0^{\pi/2} \sin \theta d\theta d\phi = 2\pi$$

while

$$\int_{\Omega} X d\Omega = \int_{-\pi}^{\pi} \int_0^{\pi/2} (1/2) \sin 2\theta d\theta d\phi = \pi$$

The latter result will be used in the discussion of perfectly diffuse reflectance.

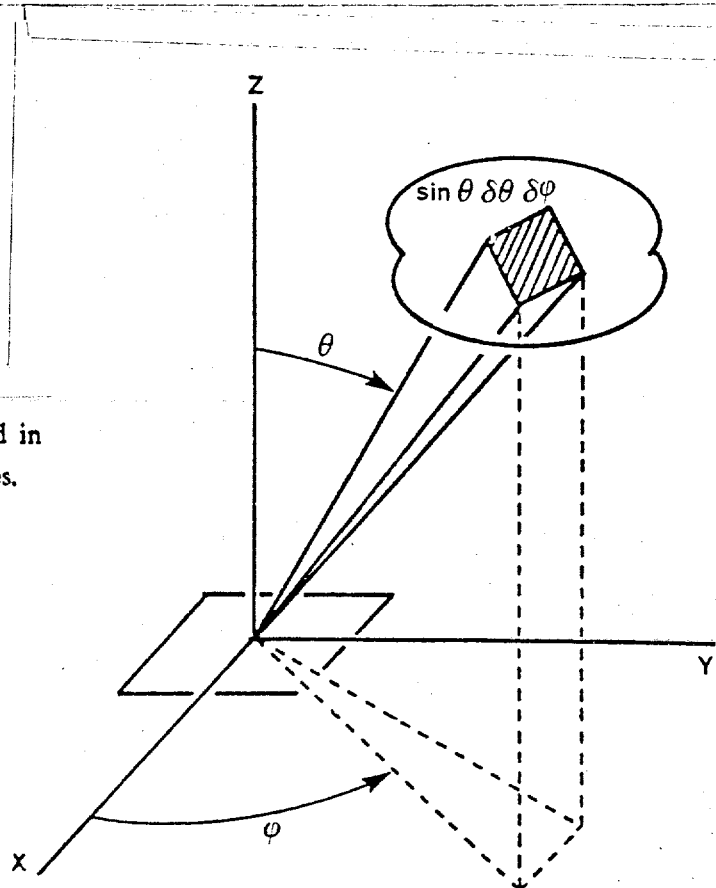


FIGURE 5: Polar and azimuth angles used in double integrals over specified solid angles.

## §6. PERFECTLY DIFFUSE REFLECTANCE

A perfectly diffuse or "lambertian" surface appears equally bright from all directions, regardless of how it is irradiated, and reflects all incident light [43]. Thus the reflected radiance is isotropic, that is,  $L_r$  is constant, with the same value for all directions  $(\theta_r, \phi_r)$ . Also, the integral of reflected radiance over the hemisphere above the surface must equal the irradiance  $E$ . This implies that the BRDF for this ideal surface,  $f_{r,id}$ , is constant, and that the radiant exitance  $M$  equals the irradiance  $E$ . If the reflected radiance is  $L_r$ , then the radiant exitance can be found by integration:

$$M = \int_{\Omega_r} L_r d\Omega_r = L_r \pi$$

From this one finds that

$$f_{r,id} = L_r/E_i = L_r/M = 1/\pi$$

If we have an extended source with radiance  $L_i$ , then the irradiance on the surface due to a small portion of solid angle  $d\omega_i$  lying in the direction  $(\theta_i, \phi_i)$  is

$$dE_i(\theta_i, \phi_i) = L_i(\theta_i, \phi_i) \cos \theta_i d\omega_i.$$

The reflected radiance is then

$$L_r = (1/\pi) \int_{\omega} L_i(\theta_i, \phi_i) \cos \theta_i d\omega_i$$

This is a form of Lambert's cosine law.

## §7. COLLIMATED SOURCES AND THE DIRAC DELTA-FUNCTION

Not all sources are extended. One way to deal with sources that are highly collimated is to treat them as limiting cases of extended sources, with the distribution tending towards an impulse or delta-function. If this is to be expressed in a coordinate system of polar and azimuth angles, one has to take into account the non-uniform spacing of coordinates. Consider a collimated source which produces an irradiance  $E_0$  on a surface oriented orthogonally to the direction  $(\theta_0, \phi_0)$  of its rays. Clearly the radiance  $L_i$  of this source should be zero except for this direction. The product of Dirac delta functions,  $\delta(\theta_i - \theta_0) \cdot \delta(\phi_i - \phi_0)$ , will be a useful ingredient of the formula expressing  $L_i$  as a function of the angles. One must insure, however, that the

irradiance on a surface lying orthogonal to the rays equals  $E_0$ , that is,

$$E_0 = \int_{-\pi}^{\pi} \int_0^{\pi/2} L_i \sin \theta_i d\theta_i d\phi_i.$$

Clearly this can be accomplished if

$$L_i = E_0 \delta(\theta_i - \theta_0) \delta(\phi_i - \phi_0) / \sin \theta_0$$

This is called the "double-delta" representation of source radiance for a collimated source. It can also be written in an alternate form using the identity

$$\delta[f(x) - f(x_0)] = \delta(x - x_0) / f'(x_0).$$

where  $f'(x_0)$  is the derivative of  $f(x)$  evaluated at  $x = x_0$ , provided that  $f(x)$  has an inverse in the domain of interest. (This identity can be confirmed by integrating each side with respect to  $x$  over the relevant interval.) Then,

$$L_i = E_0 \delta(\cos \theta_i - \cos \theta_0) \delta(\phi_i - \phi_0).$$

## §8. PERFECTLY SPECULAR REFLECTANCE

A perfectly specular or "mirror-like" surface reflects light rays in such a way that the exitant angle  $\theta_r$  equals the incident angle  $\theta_i$  and that the incident and reflected ray lie in a plane containing the surface normal. The reflected radiance of a surface patch in the direction  $(\theta_r, \phi_r)$  is simply the source radiance in the corresponding reflected direction. That is,

$$L_r(\theta_r, \phi_r) = L_i(\theta_r, \phi_r + \pi)$$

The surface thus forms a virtual image of the source. From the definition of the BRDF, we see that

$$L_r = \int f_r dE_i = \int_{\Omega_i} f_r L_i d\Omega_i$$

That is,

$$L_r = \int_{-\pi}^{\pi} \int_0^{\pi/2} f_r L_i \cos \theta_i \sin \theta_i d\theta_i d\phi_i$$

We can satisfy the conditions stated above if we let

$$f_{r, is} = \delta(\theta_i - \theta_r) \delta(\phi_i - \phi_r + \pi) / (\sin \theta_i \cos \theta_i)$$

This is called the "double-delta" form of the BRDF for perfectly specular reflectance. Using the identity mentioned in the last section, we can write this in an alternate form [43]:

$$f_{r,is} = 2 \delta(\sin^2 \theta_r - \sin^2 \theta_i) \delta(\phi_r - \phi_i + \pi)$$

## §9. ANALYSIS OF IMAGE-FORMING SYSTEM

We will now analyze a simple image-forming system (Fig. 6). We assume that the device is properly focused; that is, those rays originating from a particular point on the object which pass through the entrance aperture are deflected to meet at a single point in the image plane. Similarly, rays originating in the infinitesimal area  $dA_0$  on the object's surface are projected into some area  $dA_p$  in the image plane and no rays from other portions of the object's surface will reach this area of the image. Further, we assume that there is no "vignetting," that is, the entrance aperture is a constant circle of diameter  $d$  and does not become occluded for directions which make a larger angle with the optical axis. The effect of vignetting on image irradiance will be considered later.

The exposure of film in a camera is proportional to image irradiance,  $E_p$ , and gray-levels in a digital imaging system are quantized measurements of image irradiance. In order to calculate image irradiance we must first determine the flux  $d\Phi_L$  passing through the entrance aperture arriving from the patch of area  $dA_0$  on the object.

$$d\Phi_L = dA_0 \int_{\Omega_r} L_r d\Omega_r$$

where  $\Omega_r$  is the projected solid angle subtended by the aperture. We will also need to know the area  $dA_p$  of the image of the patch, since image irradiance  $E_p$  is the flux per unit area:

$$E_p = d\Phi_L / dA_p$$

If  $\theta_r'$  is the angle between the normal on the surface and the line to the entrance aperture nodal point, while  $\alpha$  is the angle between this line and the optical axis, then, by equating solid angles,

$$(dA_0 \cos \theta_r') / f_0^2 = (dA_p \cos \alpha) / f_p^2$$

Consequently,

$$E_p = (f_0 / f_p)^2 \cos \alpha \int_{\omega_r} L_r (\cos \theta_r / \cos \theta_r') d\omega_r$$

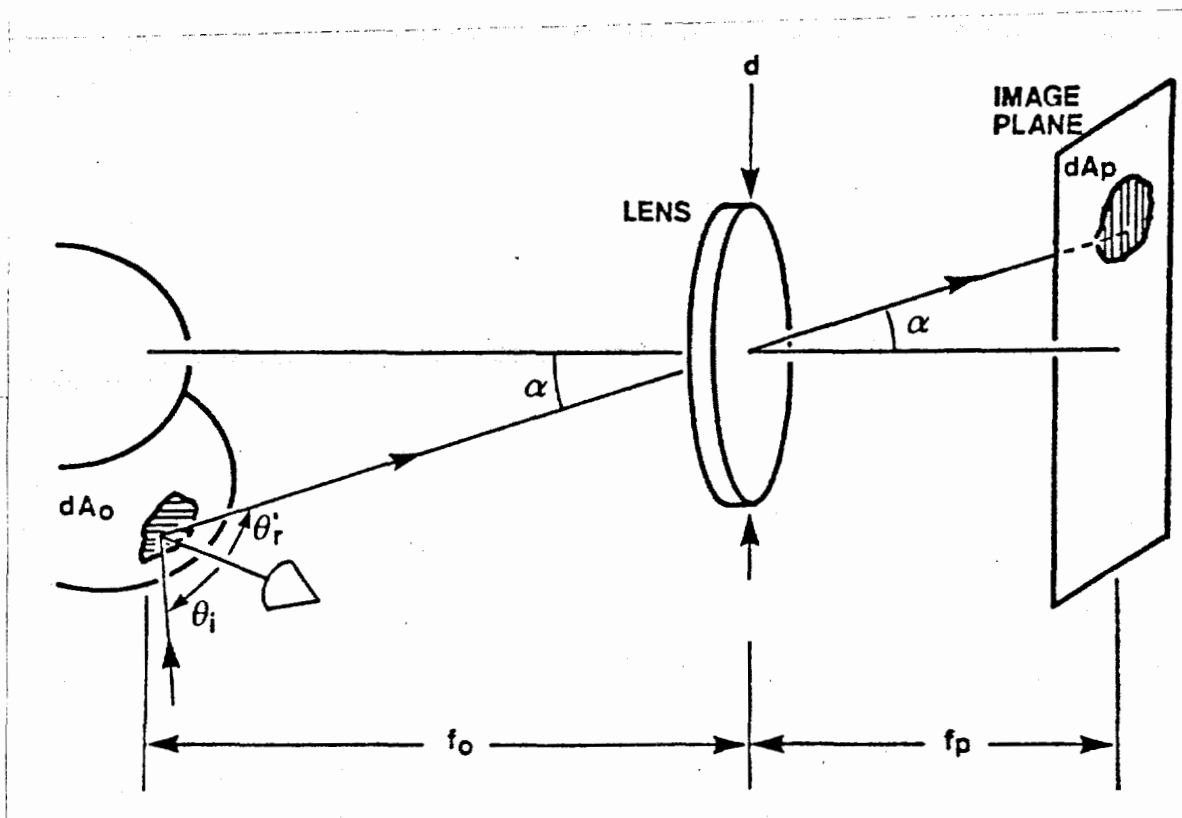


FIGURE 6: A simple image forming system. Light collected by the lens from the surface patch of area  $dA_0$  is projected into the image patch of area  $dA_p$ .

Here the integral is over the solid angle occupied by the entrance aperture as seen from the patch on the surface. If we assume that the lens is small relative to its distance from the object,  $\theta_r$  is approximately the same as  $\theta_r'$ , and the ratio of their cosines is unity. Furthermore, the reflected radiance  $L_r$  will then tend to be constant and can be removed from inside the integral. The solid angle occupied by the lens as seen from the surface patch is approximately equal to the foreshortened area  $(\pi/4) d^2 \cos \alpha$ , divided by the distance  $(f_0/\cos \alpha)$  squared. Finally, one obtains the well-known result,

$$E_p = L_r (\pi/4) (d/f_p)^2 \cos^4 \alpha$$

That is, image irradiance is proportional to scene radiance. The factor of proportionality is  $\pi$  divided by four times the effective f-number  $(f_p/d)$  squared, times the fourth power of the cosine of the off-axis angle,  $\alpha$ . Thus the "sensitivity" of such an imaging system is not uniform over an image, but is constant for a particular point in the image. Vignetting introduces an additional variation with image position. Ideally, an imaging device should be calibrated so that this variation in sensitivity as a function of  $\alpha$  can be removed.

Other kinds of imaging systems, such as microscopes or mechanical scanners, lead to somewhat different expressions. Generally, however, image irradiance is proportional to scene radiance in such systems too. At this point we should remember that scene radiance depends on properties of the surface layer (BRDF) and the distribution of light-sources (source radiance) since

$$L_r = \int_{\Omega_i} f_r L_i d\Omega_i$$

### §10. VIEWER-ORIENTED COORDINATE SYSTEM.

So far we have considered directions from the object to the image-forming system and to light sources in terms of a *local* coordinate system with one axis lined up with the surface normal. Such coordinate systems will vary in orientation from place to place and are thus inconvenient for the specification of global distributions such as that of source radiance. A coordinate system fixed in space will be more suitable, particularly if one of the axes is lined up with the optical axis (Fig. 7). In this *viewer-oriented* coordinate system we introduce polar angle  $\theta$  measured from the  $z$ -axis and azimuth angle  $\phi$  measured from the  $x$ -axis in the plane perpendicular to the  $z$ -axis. Here, the  $z$ -axis is parallel to the optical axis. Directions to sources of light can be given using these two angles. If the sources are far away in comparison to the size of the objects being imaged, then source radiance will be a fixed function of these angles independent of the point on the surface being considered.

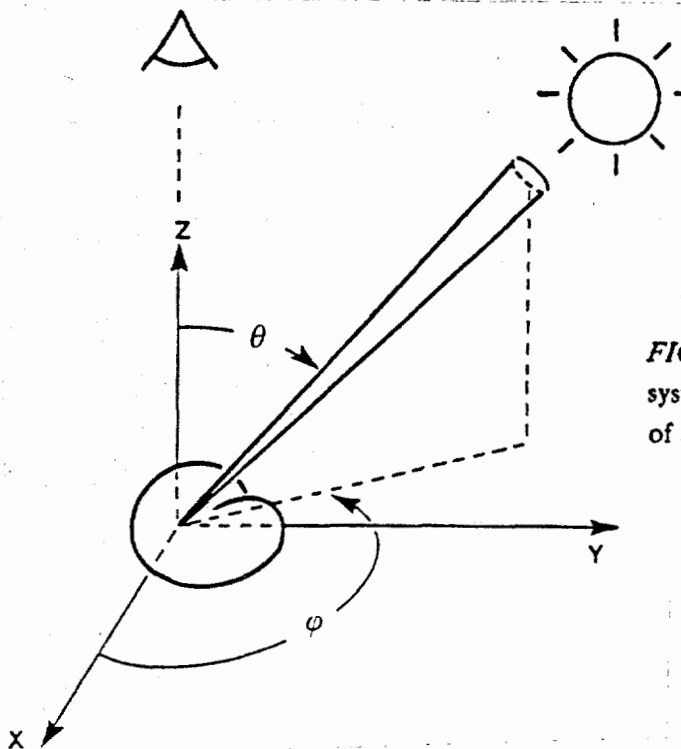


FIGURE 7: Viewer-oriented, global coordinate system useful for specification of the distribution of source radiance  $L_i$ .



## §11. THE SURFACE NORMAL

In the local coordinate system the surface normal lies along one of the axes, or equivalently, it is the direction corresponding to zero polar angle. In the viewer-oriented coordinate system the surface normal will correspond to some direction, say  $(\theta_n, \phi_n)$ . The corresponding unit vector is,

$$\mathbf{n} = (\cos \phi_n \sin \theta_n, \sin \phi_n \sin \theta_n, \cos \theta_n)$$

The surface of the object may be specified by giving "elevation"  $z$  as a function of the coordinates  $x$  and  $y$ . We can give an expression for the surface normal in terms of the first partial derivatives of  $z$  with respect to  $x$  and  $y$ , if these exist. Let the first partial derivatives be called  $p$  and  $q$ . Then the vectors  $(1, 0, p)$  and  $(0, 1, q)$  are tangent to the surface, as can be seen by considering infinitesimal steps in the  $x$  and  $y$  direction. The surface normal is perpendicular to all vectors in the tangent plane and so is parallel to the cross-product of these two:

$$(1, 0, p) \times (0, 1, q) = (-p, -q, 1)$$

Thus the unit normal can be written

$$\mathbf{n} = (-p, -q, 1) / \sqrt{1 + p^2 + q^2}$$

The following results are obtained by equating terms in the two expressions for the surface normal:

$$\sin \theta_n = \sqrt{p^2 + q^2} / \sqrt{1 + p^2 + q^2}$$

$$\cos \theta_n = 1 / \sqrt{1 + p^2 + q^2}$$

$$\sin \phi_n = -q / \sqrt{p^2 + q^2}$$

$$\cos \phi_n = -p / \sqrt{p^2 + q^2}$$

Conversely,

$$p = -\cos \phi_n \tan \theta_n$$

$$q = -\sin \phi_n \tan \theta_n$$

## §12. RELATIONSHIP BETWEEN LOCAL AND VIEWER-ORIENTED COORDINATE SYSTEMS

In order to calculate the scene radiance, we will integrate the product of the BRDF and the source radiance over all incident directions. Since the BRDF is specified in terms of the *local* coordinate system, while the distribution of source radiance is likely to be given in the *viewer-oriented* coordinate system, it will be necessary to convert between the two. Given the direction of the surface normal,  $(\theta_n, \phi_n)$ , and the direction to a portion of the source  $(\theta_s, \phi_s)$ , both specified in the viewer-oriented system (Fig. 8), we have to find the incident direction  $(\theta_i, \phi_i)$  and the exitant direction  $(\theta_r, \phi_r)$  both specified in the local system. Alternatively, given the surface normal and the incident direction we may have to find the direction to the source and the exitant direction. Note that  $\theta_r = \theta_n$  since the exitant ray lies along the z-axis in the direction towards the viewer. Further, since we have excluded anisotropic surfaces, we are only interested in the *difference* between  $\phi_r$  and  $\phi_i$ . From the relevant spherical triangle (Fig. 9) we obtain

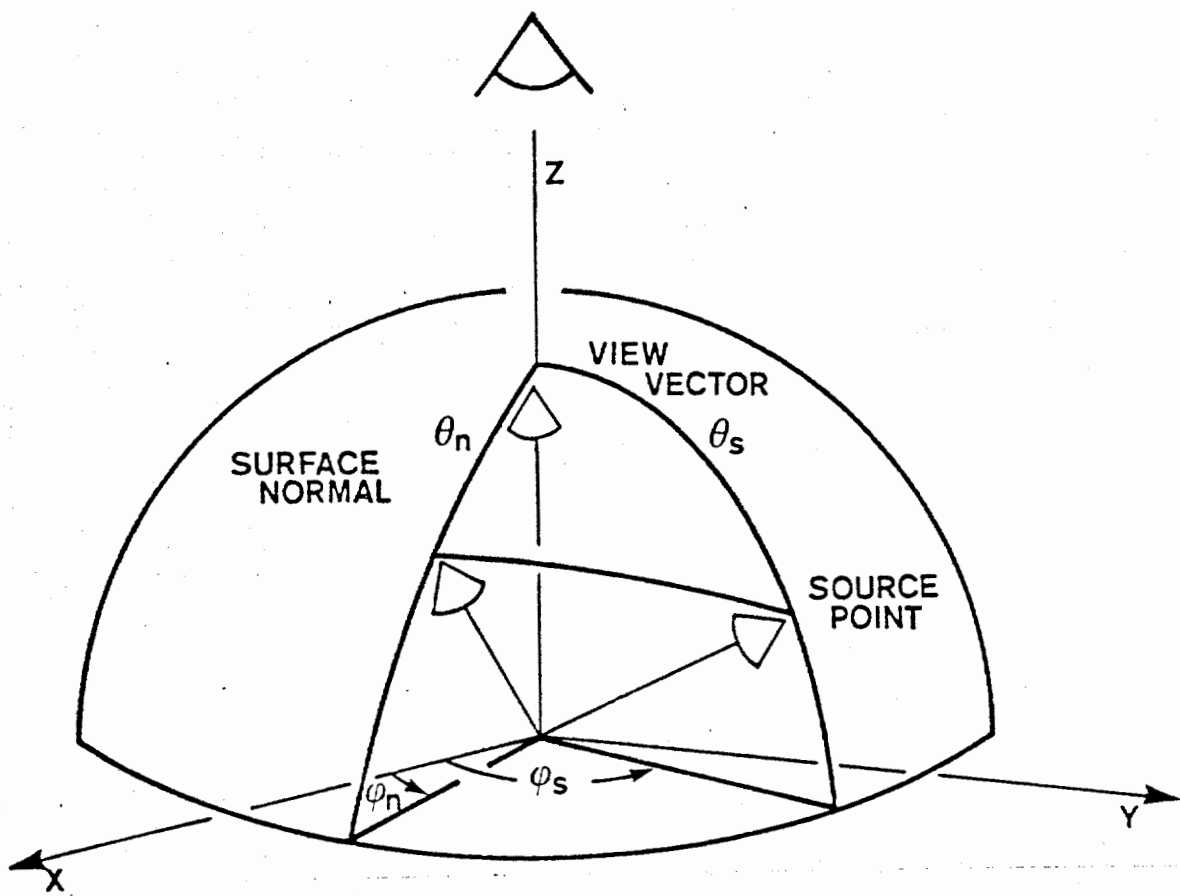


FIGURE 8: Surface normal and direction to portion of the source shown in viewer-oriented coordinate system.

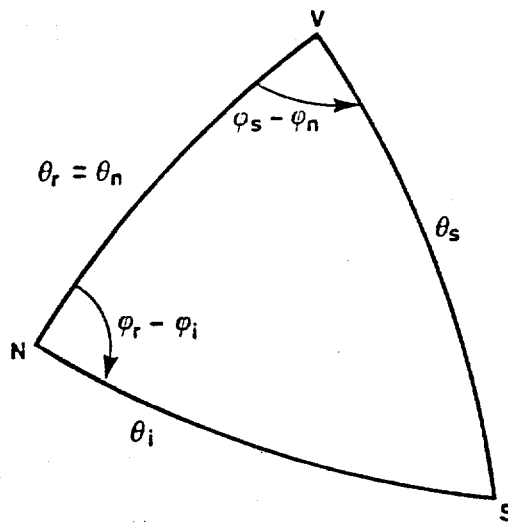


FIGURE 9: Spherical triangle extracted from previous figure and used in derivation of transformation equations between the surface-normal, local coordinate system, and the viewer-oriented, global coordinate system.

Cosine formula:

$$\cos \theta_i = \cos \theta_s \cos \theta_n + \sin \theta_s \sin \theta_n \cos (\phi_s - \phi_n)$$

Sine formula:

$$\sin \theta_i \sin (\phi_r - \phi_i) = \sin \theta_s \sin (\phi_s - \phi_n)$$

Analogue formula:

$$\sin \theta_i \cos (\phi_r - \phi_i) = \cos \theta_s \sin \theta_n - \sin \theta_s \cos \theta_n \cos (\phi_s - \phi_n)$$

The Jacobian of the transformation from  $(\theta_s, \phi_s)$  to  $(\theta_i, \phi_i)$  equals

$$(\partial \theta_i / \partial \theta_s) (\partial \phi_i / \partial \phi_s) - (\partial \theta_i / \partial \phi_s) (\partial \phi_i / \partial \theta_s) = (\sin \theta_s / \sin \theta_i).$$

(The Jacobian will be required below when converting a double integral with respect to one set of coordinates to one in terms of the other.) The above formulae allow us to find the incident direction from the source direction. Quite symmetrically, we can also obtain the source direction from the incident direction:

Cosine formula:

$$\cos \theta_s = \cos \theta_i \cos \theta_r + \sin \theta_i \sin \theta_r \cos (\phi_r - \phi_i)$$

Sine formula:

$$\sin \theta_s \sin (\phi_s - \phi_n) = \sin \theta_i \sin (\phi_r - \phi_i)$$

Analogue formula:

$$\sin \theta_s \cos (\phi_s - \phi_n) = \cos \theta_i \sin \theta_r - \sin \theta_i \cos \theta_r \cos (\phi_r - \phi_i)$$

The Jacobian of the transformation from  $(\theta_i, \phi_i)$  to  $(\theta_s, \phi_s)$  equals

$$(\partial\theta_s/\partial\theta_i) (\partial\phi_s/\partial\phi_i) - (\partial\phi_s/\partial\theta_i) (\partial\theta_s/\partial\phi_i) = (\sin \theta_i / \sin \theta_s).$$

### §13. SCENE RADIANCE

It follows from the definition of the BRDF that reflected radiance can be written as the integral

$$L_r = \int_{\Omega_i} f_r L_i d\Omega_i = \int_{\omega_i} f_r L_i \cos \theta_i d\omega_i$$

Using polar and azimuthal angles this becomes

$$L_r(\theta_n, \phi_n) = \int_{-\pi}^{\pi} \int_0^{\pi/2} f_r(\theta_i, \phi_i; \theta_r, \phi_r) L_i(\theta_s, \phi_s) \cos \theta_i \sin \theta_i d\theta_i d\phi_i$$

Here we integrate over all possible incident directions  $(\theta_i, \phi_i)$  and calculate source direction  $(\theta_s, \phi_s)$  from the given surface normal  $(\theta_n, \phi_n)$  and the incident direction. The inner integral has the limits 0 to  $\pi/2$  for  $\theta_i$ , corresponding to directions within the hemisphere visible from the surface. The integration can be extended to the full sphere of directions if the integrand is forced to be zero when  $\theta_i$  lies between  $\pi/2$  and  $\pi$ . This can be accomplished by replacing  $\cos \theta_i$  by  $\max[0, \cos \theta_i]$ . Hence

$$L_r = \int_{-\pi}^{\pi} \int_0^{\pi} f_r L_i \max[0, \cos \theta_i] \sin \theta_i d\theta_i d\phi_i$$

Since the integral now is over the full sphere of directions, it can be easily rewritten using any other set of polar and azimuth angles. Using the *viewer-oriented* coordinate system, for example, we obtain

$$L_r = \int_{-\pi}^{\pi} \int_0^{\pi} f_r L_i \max[0, \cos \theta_i] \sin \theta_s d\theta_s d\phi_s$$

That is,

$$L_r(\theta_n, \phi_n) = \int_{-\pi}^{\pi} \int_0^{\pi} f_r(\theta_i, \phi_i; \theta_r, \phi_r) L_i(\theta_s, \phi_s) \max[0, \cos \theta_i] \sin \theta_s d\theta_s d\phi_s$$

Here we integrate over all possible source directions  $(\theta_s, \phi_s)$  and calculate incident directions  $(\theta_i, \phi_i)$  from the given surface normal  $(\theta_n, \phi_n)$  and the source direction. We now have two convenient forms for the calculation of scene radiance. We proceed to calculate reflectance maps for a few simple combinations of BRDF and distributions of source radiance.

### §14a. COLLIMATED SOURCE, LAMBERTIAN REFLECTANCE

For a lambertian reflector,  $f_r = 1/\pi$ . For a collimated source,

$$L_i = E_0 \delta(\theta_s - \theta_0) \delta(\phi_s - \phi_0) / \sin \theta_0$$

where  $E_0$  is the irradiance measured perpendicular to the beam of light arriving from source direction  $(\theta_0, \phi_0)$ . Substituting into the second form of the expression for scene radiance above, we obtain

$$L_r = \int_{-\pi}^{\pi} \int_0^{\pi} (E_0/\pi) \delta(\theta_s - \theta_0) \delta(\phi_s - \phi_0) \max[0, \cos \theta_i] (\sin \theta_s / \sin \theta_0) d\theta_s d\phi_s$$

This is equal to

$$L_r = (E_0/\pi) \max[0, \cos \theta'_i]$$

where  $\theta'_i = \theta_i$  when  $\theta_s = \theta_0$  and  $\phi_s = \phi_0$ . In this case,

$$\cos \theta'_i = \cos \theta_r \cos \theta_0 + \sin \theta_r \sin \theta_0 \cos(\phi_0 - \phi_n)$$

and

$$\cos(\phi_0 - \phi_n) = \cos \phi_0 \cos \phi_n - \sin \phi_0 \sin \phi_n$$

To obtain the reflectance map, scene radiance as a function of surface gradient, we can substitute expressions in  $p$  and  $q$  for these trigonometric expressions. The result is

$$R(p, q) = (E_0/\pi) \max \left[ 0, \frac{(1 + p_0 p + q_0 q)}{\sqrt{1 + p^2 + q^2} \sqrt{1 + p_0^2 + q_0^2}} \right]$$

where

$$\begin{aligned} p_0 &= -\cos \phi_0 \tan \theta_0 \\ q_0 &= -\sin \phi_0 \tan \theta_0 \end{aligned}$$

A surface with gradient  $(p_0, q_0)$  is normal to the direction of the incident light rays.

### §14b. UNIFORM SOURCE, LAMBERTIAN REFLECTANCE

A uniform source has constant incident radiance. Let  $L_i = L_0$ . Again, for a lambertian reflector,  $f_r = 1/\pi$ . Substituting into the first form of the expression for scene radiance, we obtain

$$L_r = \int_{-\pi}^{\pi} \int_0^{\pi/2} (L_0/\pi) \cos \theta_i \sin \theta_i d\theta_i d\phi_i$$

This becomes

$$L_r = L_0 \int_0^{\pi/2} \sin 2\theta_i d\theta_i = L_0$$

Not surprisingly, the reflected radiance is independent of the surface orientation in this case.

### §14c. HEMISPHERICAL UNIFORM SOURCE, LAMBERTIAN REFLECTANCE

A hemispherical uniform source is described by

$$\begin{aligned} L_i(\theta_s, \phi_s) &= L_0 & \text{for } \theta_s < \pi/2 \\ L_i(\theta_s, \phi_s) &= 0 & \text{for } \theta_s > \pi/2 \end{aligned}$$

In order to evaluate the double integral for scene radiance, it is necessary to know the value  $\theta'_i$  of the incident angle  $\theta_i$ , which corresponds to the "horizon" of the "sky," that is,  $\theta_s = \pi/2$ . From the coordinate transformation equations one can easily see that

$$\cot \theta'_i = -\tan \theta_r \cos(\phi_r - \phi_i)$$

For  $\phi_r - \pi/2 < \phi_i < \phi_r + \pi/2$ , the horizon cutoff only occurs for  $\theta'_i > \pi/2$  and can be ignored, since the inner integral is from  $\theta_i = 0$  to  $\theta_i = \pi/2$  only. For the other half of the range of  $\phi_i$ , this cutoff must be considered. Now,

$$L_r = \int_{-\pi}^{\pi} \int_0^{\pi/2} f_r L_i \cos \theta_i \sin \theta_i d\theta_i d\phi_i$$

so,

$$L_r = (L_0/\pi) \int_{-\pi}^{\pi} \int_0^{\min[\theta'_i, \pi/2]} \cos \theta_i \sin \theta_i d\theta_i d\phi_i$$

Letting  $\phi = \phi_i - \phi_r$  and  $\phi' = \phi_i - \phi_r + \pi$ , we can split the outer integral,

$$L_r = (L_0/\pi) \int_{-\pi/2}^{\pi/2} \int_0^{\pi/2} \cos \theta_i \sin \theta_i d\theta_i d\phi + (L_0/\pi) \int_{-\pi/2}^{\pi/2} \int_0^{\theta_i'} \cos \theta_i \sin \theta_i d\theta_i d\phi'$$

Now,

$$\int_0^{\pi/2} \cos \theta_i \sin \theta_i d\theta_i = 1/2$$

so the first term is simply  $L_0/2$ . Next, note that

$$\int_0^{\theta_i'} \cos \theta_i \sin \theta_i d\theta_i = (1 - \cos 2\theta_i')/4 = \sin^2 \theta_i'/2$$

where, since  $\cot \theta_i' = -\tan \theta_r \cos (\phi_r - \phi_i)$ ,

$$\sin^2 \theta_i' = 1/[1 + \tan^2 \theta_r \cos^2 (\phi_r - \phi_i)]$$

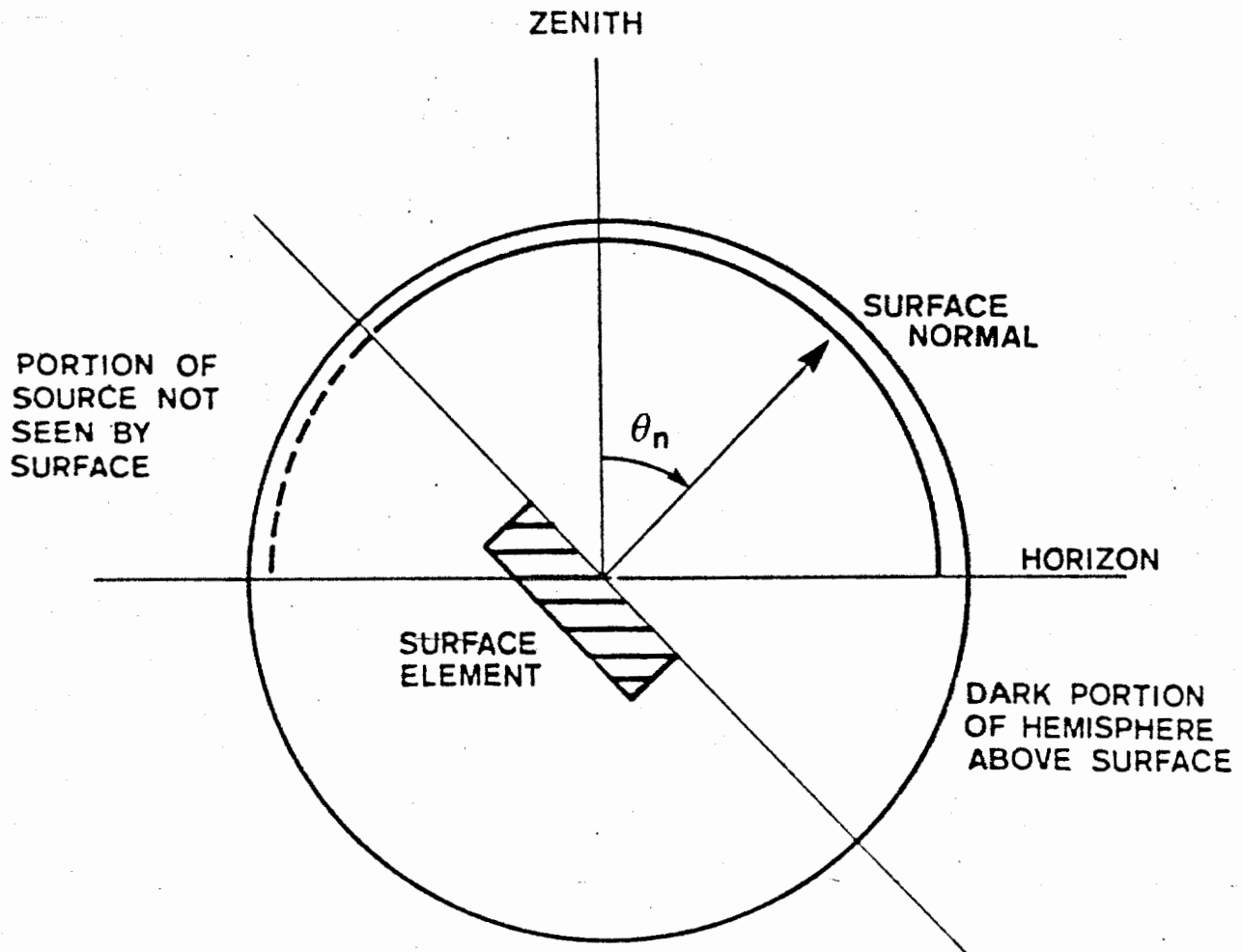


FIGURE 10: Cross-section through uniform hemispherical source and surface element, illustrating horizon cutoff and portion of extended source not visible from surface.

The second term thus becomes

$$(L_0/2\pi) \int_{-\pi/2}^{\pi/2} 1/[1 + \tan^2 \theta_r \cos^2 \phi'] d\phi'$$

which equals

$$(L_0/2\pi) [\cos \theta_r \tan^{-1} (\cos \theta_r \tan \phi)]_{-\pi/2}^{\pi/2} = (L_0/2) \cos \theta_r$$

Adding up the two terms we finally get

$$L_r(\theta_n, \phi_n) = (L_0/2) (1 + \cos \theta_n) = L_0 \cos^2 (\theta_n/2)$$

This is the result found by Brooks [44]. From it the reflectance map can be found immediately:

$$R(p, q) = (E_0/2) (1 + 1/\sqrt{1 + p^2 + q^2})$$

### §15a. COLLIMATED SOURCE, SPECULAR REFLECTANCE

For specular surfaces,

$$f_r = \delta(\theta_i - \theta_r) \delta(\phi_i - \phi_r + \pi) / (\sin \theta_i \cos \theta_i)$$

Using the source radiance from §14a above, and the first form of the expression for scene radiance, we obtain

$$L_r = \int_{-\pi}^{\pi} \int_0^{\pi/2} (L_0/\sin \theta_0) \delta(\theta_i - \theta_r) \delta(\phi_i - \phi_r + \pi) \delta(\theta_s - \theta_0) \delta(\phi_s - \phi_0) d\theta_i d\phi_i$$

That is,

$$L_r = L_0 \delta(\theta_s' - \theta_0) \delta(\phi_s' - \phi_0) / \sin \theta_0$$

where  $\theta_s'$  and  $\phi_s'$  are the values of  $\theta_s$  and  $\phi_s$  corresponding to  $\theta_i = \theta_r$  and  $\phi_i = \phi_r + \pi$ . Using the equations for the coordinate transformations, one finds that  $\theta_s' = 2\theta_r$  and  $\phi_s' = \phi_n$ . Thus,

$$L_r = L_0 \delta(2\theta_r - \theta_0) \delta(\phi_n - \phi_0) / \sin \theta_0$$

and finally,

$$L_r(\theta_n, \phi_n) = (L_0/2) \delta(\theta_n - \theta_0/2) \delta(\phi_n - \phi_0) / \sin \theta_0$$



To express this as a function of  $p$  and  $q$  we have to remember that

$$\delta[f(x, y) - f(x_0, y_0)] \delta[g(x, y) - g(x_0, y_0)] = \delta(x - x_0) \delta(y - y_0) / J(x_0, y_0)$$

where  $J(x, y)$  is the Jacobian of the transformation from  $(x, y)$  to  $(f, g)$ , (provided this transformation has an inverse in the region of interest):

$$J(x, y) = (\partial f / \partial x) (\partial g / \partial y) - (\partial f / \partial y) (\partial g / \partial x)$$

The Jacobian of the transformation from  $(p, q)$  to  $(\theta_n, \phi_n)$  is

$$J(p, q) = 1 / [ \sqrt{p^2 + q^2} (1 + p^2 + q^2) ]$$

Let

$$\begin{aligned} p_1 &= -\cos \phi_0 \tan \theta_0 / 2 \\ q_1 &= -\sin \phi_0 \tan \theta_0 / 2. \end{aligned}$$

Then, noting that  $\sin \theta_0 = 2 \sin(\theta_0/2) \cos(\theta_0/2)$ , one can write

$$\sin \theta_0 = 2 \sqrt{p_1^2 + q_1^2} / (1 + p_1^2 + q_1^2)$$

and therefore,

$$R(p, q) = (E_0/4) \delta(p - p_1) \delta(q - q_1) (1 + p_1^2 + q_1^2)^2$$

Thus, a surface element with gradient  $(p_1, q_1)$  is oriented to specularly reflect the collimated source towards the viewer. This gradient can be related to the gradient  $(p_0, q_0)$  introduced earlier:

$$\begin{aligned} p_1 &= p_0 (\sqrt{1 + p_0^2 + q_0^2} - 1) / (p_0^2 + q_0^2) \\ q_1 &= q_0 (\sqrt{1 + p_0^2 + q_0^2} - 1) / (p_0^2 + q_0^2) \end{aligned}$$

When the point  $(p_0, q_0)$  is not far from the origin, then  $(p_1, q_1)$  is approximately midway between the origin and  $(p_0, q_0)$ .

### §15b. UNIFORM SOURCE, SPECULAR REFLECTANCE

It is easy to see that for a specular surface under a uniform source, the scene radiance will be constant and equal to the source radiance.

$$L_r = L_0$$

This is the same result as the one we obtained for the uniform source and lambertian reflectance. Thus a diffuse surface appears just as bright as a specular surface if both are viewed with uniform illumination. In fact, all surfaces reflecting the same fraction,  $\rho$  say, of the total incident light will appear equally bright under this illumination condition.

### §15c. HEMISPHERICAL UNIFORM SOURCE, SPECULAR REFLECTANCE

In this case,

$$\begin{aligned} L_r(\theta_n, \phi_n) &= L_0 & \text{for } \theta_n < \pi/4 \\ L_r(\theta_n, \phi_n) &= 0 & \text{for } \theta_n > \pi/4 \end{aligned}$$

The reflectance map is

$$\begin{aligned} R(p, q) &= L_0 & \text{for } p^2 + q^2 < 1 \\ R(p, q) &= 0 & \text{for } p^2 + q^2 > 1 \end{aligned}$$

### SUMMARY AND CONCLUSIONS

We have shown that image irradiance is proportional to scene radiance and that scene radiance depends on surface orientation. The reflectance map gives scene radiance as a function of the gradient. It can be calculated from the bidirectional reflectance-distribution function (BRDF) and the distribution of source radiance. Several special cases were worked out in detail. Each could have been developed more easily by a direct method, but was obtained from the general expression for scene radiance to illustrate the technique. The general expression allows one to find the reflectance map even if the source radiance distribution or the BRDF is only given numerically.

## ACKNOWLEDGEMENTS

The authors would like to thank H.-H. Nagel, B. Neumann, B. Radig and L. Dreschler of the University of Hamburg, who helped debug some of the ideas. Discussions with M. Brady and M. Brooks of the University of Essex were very helpful. Thanks go to P. Winston and K. Ikeuchi for helping to proofread the manuscript. We are also grateful for text preparation by Blenda Horn and drawings by Karen Prendergast.

## REFERENCES

- [1] Diggelen, J. van (1951) "A Photometric Investigation of the Slopes and Heights of the Ranges of Hills in the Maria of the Moon," *Bulletin of the Astronomical Institute of the Netherlands*, Vol. 11, No. 423, July 1951.
- [2] Rindfleisch, T. (1966) "Photometric Method for Lunar Topography," *Photogrammetric Engineering*, Vol. 32, March 1966, pp. 262-276.
- [3] Horn, B. K. P. (1975) "Determining Shape from Shading," Chapter 4, in Winston, P. H. (Ed) *The Psychology of Computer Vision*, McGraw-Hill, New York.
- [4] Horn, B. K. P. (1977) "Understanding Image Intensities," *Artificial Intelligence*, Vol. 8, No. 11, pp 201-231.
- [5] Woodham, R. J. (1977) "A Cooperative Algorithm for Determining Surface Orientation from a Single View," *Proc. 5th Int. Joint Conf. on Artif. Intell.*, M.I.T., Cambridge, Massachusetts, August 1977, pp 635-641.
- [6] Woodham, R. J. (1978) "Reflectance Map Techniques for Analyzing Surface Defects in Metal Castings," TR-457, Artificial Intelligence Laboratory, M.I.T., Cambridge, Massachusetts.
- [7] Woodham, R. J. (1978) "Photometric Stereo: A Reflectance Map Technique for Determining Surface Orientation from Image Intensity", *Proceedings of SPIE's 22nd Annual Technical Symposium*, Vol. 155, August 1978, pp. 136-143.
- [8] Horn, B. K. P., Woodham, R. J., and Silver, W. N. (1978) "Determining Shape and Reflectance Using Multiple Images," A.I. Laboratory Memo 490, M.I.T., Cambridge, Massachusetts. August 1978.
- [9] Gilpin, F. H. (1910) "Effect of the variation of the incident angle on the coefficients of diffuse reflection," *Trans. Illum. Eng. Soc.*, Vol. 5, pp 854-873.

- [10] Knowles Middleton, W. E. and Mungall, A. G. (1952) "The luminous directional reflectance of snow," *Journal of the Optical Society of America*, Vol. 42, No. 8, August 1952, pp 572-579.
- [11] Fedoretz, V. A. (1952) "Photographic Photometry of the Lunar Surface," *Publ. Kharkov Obs.*, Vol. 2, pp 49-172.
- [12] Van Diggelen, J. (1959) "Photometric Properties of Lunar Crater Floors," *Rech. Obs. Utrecht*, Vol. 14, pp 1-114.
- [13] Minnaert, M. (1961) "Photometry of the Moon," in *Planets and Satellites*, G. Kuiper and B. Middlehurst (eds), Vol. 3, Univ. of Chicago Press, Chicago, pp 213-248.
- [14] Fesenkov, V. (1962) "Photometry of the Moon," in *Physics and Astronomy of the Moon*, Z. Kopal (ed), Academic Press, New York, pp 99-130.
- [15] Hapke, B. and Van Horn, H. (1963) "Photometric Studies of Complex Surfaces, with Applications to the Moon," *Journal of Geophysical Research*, Vol. 68, No. 15, pp 4545-4570.
- [16] De Vaucouleurs, G. (1964) "Geometric and Photometric Parameters of the Terrestrial Planets," *ICARUS*, Vol. 3, pp 187-235.
- [17] Van Diggelen, J. (1965) "The radiance of lunar objects near opposition," *Planetary Space Science*, Vol. 13, pp 271-279.
- [18] Oetking, P. (1966) "Photometric Studies of Diffusely Reflecting Surfaces with Applications to the Brightness of the Moon," *Journal of Geophysical Research*, Vol. 71, No. 10, May 1966, pp 2505-2515.
- [19] Rennilson, J. J., Holt, H. E. and Morris, E. C. (1968) "In Situ Measurements of the Photometric Properties of an Area on the Lunar Surface," *Journal of the Optical Society of America*, Vol. 58, No. 6, June 1968, pp 747-755.
- [20] Patterson, E. M., Sheldon, C. E. and Stockton, B. H. (1977) "Kubelka-Munk optical properties of a barium sulfate white reflectance standard," *Applied Optics*, Vol. 16, No. 3, March 1977, pp 729-732.
- [21] Tucker, C. J. (1977) "Asymptotic nature of grass canopy spectral reflectance," *Applied Optics*, Vol. 16, No. 5, May 1977, pp 1151-1156.

- [22] Minnaert, M. (1941) "The Reciprocity Principle in Lunar Photometry," *Astrophysical Journal*, Vol. 93, pp 403-410.
- [23] Van de Hulst, H. C. (1957) *Light Scattering by Small Particles*, John Wiley and Sons, New York.
- [24] Hapke, B. W. (1963) "A Theoretical Photometric Function for the Lunar Surface," *Journal of Geophysical Research*, Vol. 68, No. 15, August 1963, pp 4571-4586.
- [25] Melamed, N. T. (1963) "Optical Properties of Powders. Part I. Optical Absorption Coefficients and the Absolute Value of Diffuse Reflectance. Part II. Properties of Luminescent Powders," *Journal of Applied Physics*, Vol. 34, No. 3, March 1963, pp. 560-570.
- [26] Hapke, B. (1966) "An Improved Theoretical Lunar Photometric Function," *The Astronomical Journal*, Vol. 71, No. 5, June 1966, pp 333-339.
- [27] Torrance, K. E., Sparrow, E. M. and Birkebak, R. C. (1966) "Polarization, directional distribution, and off-specular peak phenomena in light reflected from roughened surfaces," *Journal of the Optical Society of America*, Vol. 56, No. 7, July 1966, pp 916-925.
- [28] Torrance, K. E. and Sparrow, E. M. (1967) "Theory for off-specular reflection from roughened surfaces," *Journal of the Optical Society of America*, Vol. 57, No. 9, September 1967, pp 1105-1114.
- [29] Trowbridge, T. S. and Reitz, K. P. (1975) "Average irregularity representation of a rough surface for ray reflection", *Journal of the Optical Society of America*, Vol. 65, No. 5, May 1975, pp 531-536.
- [30] Simmons, E. L. (1975) "Diffuse reflectance spectroscopy: a comparison of the theories," *Applied Optics*, Vol. 14, No. 6, June 1975, pp 1380-1336.
- [31] Simmons, E. L. (1975) "A refinement of the simplified particle model theory of diffuse reflectance spectroscopy," *Optica Acta*, Vol. 22, No. 1, pp 71-77.
- [32] Simmons, E. L. (1975) "Modification of the particle-model theory of diffuse reflectance properties of powdered samples," *Journal of Applied Physics*, Vol. 46, No. 1, January 1975, pp 344-348.
- [33] Simmons, E. L. (1976) "Particle model theory of diffuse reflectance: effect of nonuniform particle size," *Applied Optics*, Vol. 15, No. 3, March 1976, pp 603-604.

- [34] Tucker, C. J. and Garratt, M. W. (1977) "Leaf optical system modelled as a stochastic process," *Applied Optics*, Vol. 16, No. 3, March 1977, pp 635-642.
- [35] Plass, G. N., Kattawar, G. W. and Guinn Jr., J. A. (1977) "Isophotes of sunlight glitter on a wind-ruffled sea," *Applied Optics*, Vol. 16, No. 3, March 1977, pp 643-653.
- [36] Gouraud, H. (1971) "Computer display of curved surfaces," Technical Report 113, UTEC-CSC-71, Computer Science, University of Utah, Salt Lake City, Utah.
- [37] Bui Tuong-Phong (1973) "Illumination for computer-generated images," Technical Report 129, UTEC-CSC-73, Computer Science, University of Utah, Salt Lake City, Utah.
- [38] Blinn, J. F. (1977) "Models of light reflection for computer synthesized pictures," *SIGGRAPH '77, Proc. ACM, Computer Graphics*, Vol. 11, No. 2, July 1977, pp 192-198.
- [39] Wendlandt, W. W. and Hecht, H. G. (1966) *Reflectance Spectroscopy*, Interscience, New York.
- [40] Wendlandt, W. W. (ed) (1968) *Modern Aspects of Reflectance Spectroscopy*, Plenum, New York.
- [41] Kortuem, G. (1969) *Reflectance Spectroscopy*, trans. by J. E. Lohr, Springer-Verlag, Berlin.
- [42] Spencer, D. E. and Gaston, E. G. (1975) "Current definitions of reflectance," *Journal of the Optical Society of America*, Vol. 65, No. 10, October 1975, pp 1129-1132.
- [43] Nicodemus, F. E., Richmond, J. C. and Hsia, J. J., Ginsberg, I. W. and Limperis, T. (1977) "Geometrical Considerations and Nomenclature for Reflectance," NBS Monograph 160, National Bureau of Standards, U. S. Department of Commerce, Washington, D. C., October 1977.
- [44] Brooks, M. J. (1978) "Investigating the Effects of Planar Light Sources," CSM 22, Dept. of Computer Science, Essex University, Colchester, England.